Electronic Supplementary Information (ESI)

Interaction of graphene-related materials with human intestinal cells: an *in vitro* approach

M. Kucki[a], P. Rupper[b], C. Sarrieu[c], M. Melucci[d], E. Treossi[d], A. Schwarz[e], V. León[f], A. Kraegeloh[e], E. Flahaut[c], E. Vázquez[f], V. Palermo[d], P. Wick[a]

a. Laboratory for Particles-Biology Interactions, Swiss Federal Laboratories for Materials Science and Technology (Empa), Lerchenfeldstrasse 5, CH-9014 St. Gallen, Switzerland
b. Laboratory for Advanced Fibers, Swiss Federal Laboratories for Materials Science and Technology (Empa), Lerchenfeldstrasse 5, CH-9014 St. Gallen, Switzerland
c. Université de Toulouse; CNRS, UPS, INP; Institut Carnot CIRIMAT; 118, route de Narbonne, F-31062 Toulouse Cedex 9, France
d. Istituto per la Sintesi Organica e la Fotoreattività, Consiglio Nazionale delle Richerche (CNR), Via P. Gobetti 101, 40129 Bologna, Italy
e. Nano Cell Interactions, INM - Leibniz Institute for New Materials, Campus D 2.2, D-66123 Saarbruecken, Germany
f. Departamento de Química Orgánica, Facultad de Ciencias y Tecnologías Químicas-IRICA, Universidad de Castilla-La Mancha, 13071 Ciudad Real, Spain

Further characterization details of applied GRM:

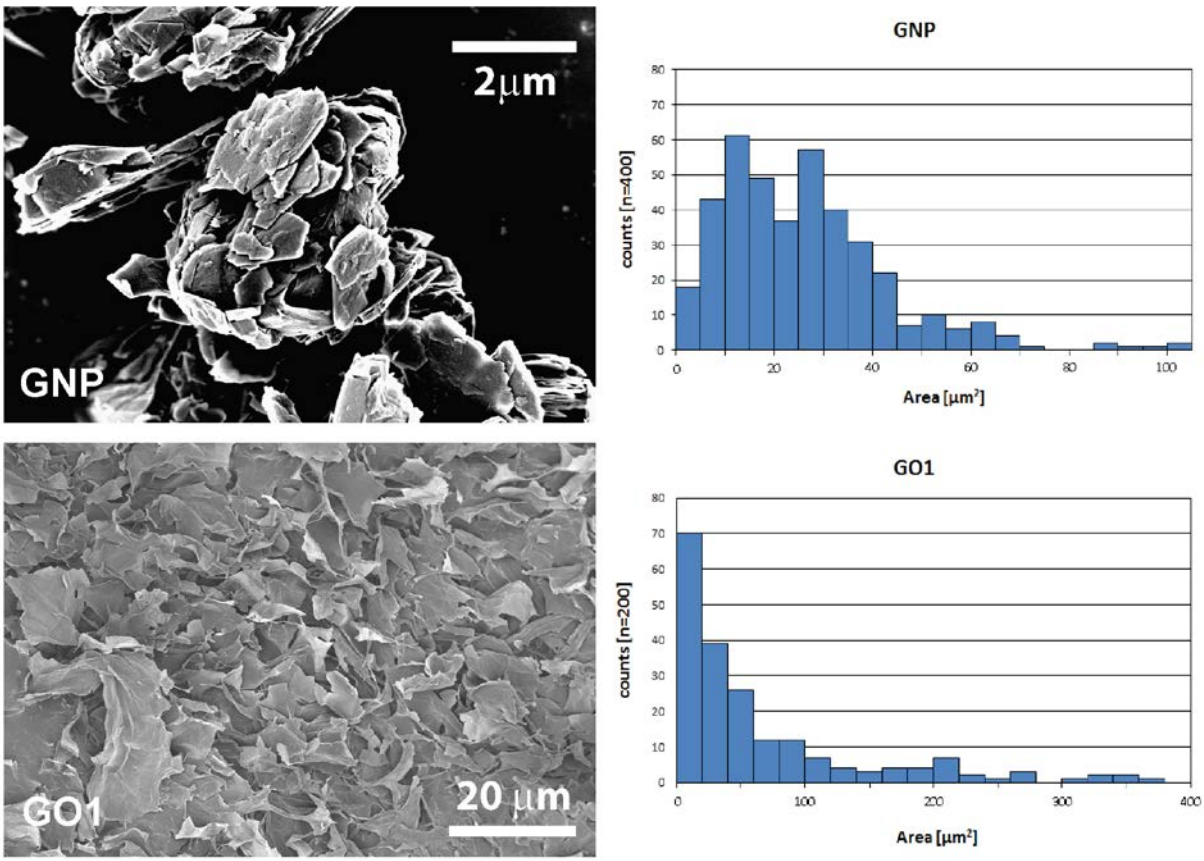

Figure S1: left: SEM images of GNP (top) and GO1 (bottom) powder as received. Right: Estimation of the size distribution of GO1 sheets and GNP aggregates presented as area in μm^2. Area was determined by microscope image analysis of GRM after dispersion in complete cell culture medium and sedimentation on glass substrate. GNP were already stacked and fused to larger aggregates in the received powder. Obtained values can only be regarded as an estimation of the size, e.g. as wrinkles, folds and some aggregation of GO1 sheets cannot be prevented in aqueous media.

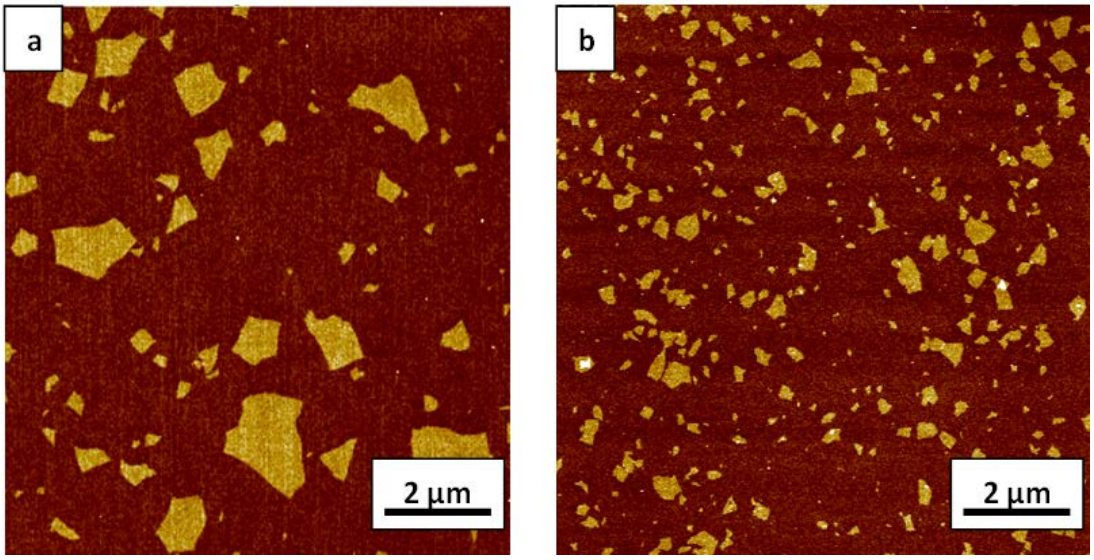

Figure S2: AFM images of a) GO2 and b) GO3 flakes obtained by spin-coating of graphene oxide solution sonicated respectively 2h or 20 hours.

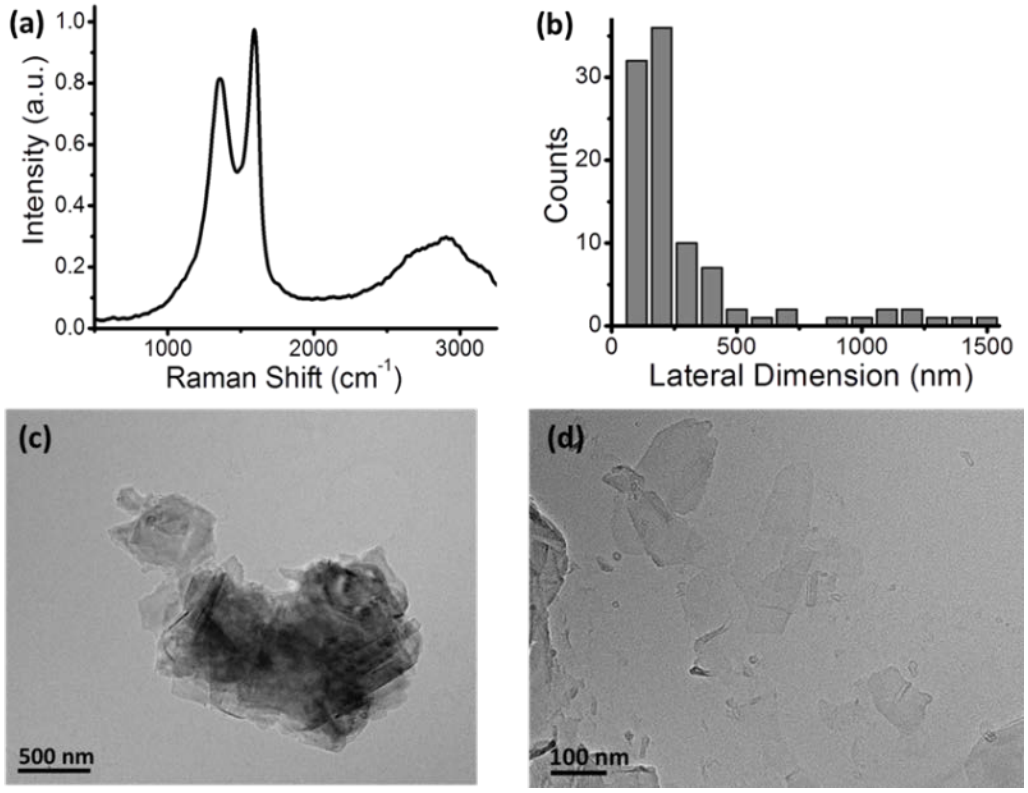

Figure S3: (a) Raman spectra of GO4 at 532 nm wavelength, (b) Lateral size distribution and (c, d) TEM images of GO4.

Table S4a: Zeta-(ζ)-Potential of applied GRM

Graphene-related material (GRM)	Zeta-(ζ)-potential (mV) in ultra-pure water with 1 mM potassium chloride (KCl) background electrolyte	Zeta-(ζ)-potential (mV) Re-dispersed in ultra-pure water after incubation in cell culture medium (incl. 10% FCS)
GO1 as received	-39.4 ± 1.3	-24.1 ± 1.1
GO1 acid-treated	-39.7 ± 3.7	-23.4 ± 2.2
GO2	-44.0 ± 0.2	-30.8 ± 1.1
GO3	-43.9 ± 1.4	-28.8 ± 0.3
GO4	-37.7 ± 0.4	-26.6 ± 0.6
GNP** as received	-62.6 ± 1.9	-25.0 ± 0.5
GNP acid-treated	-50.2 ± 1.7	-27.4 ± 0.2

** contains sodium cholate

The zeta-(ζ)-potential of dispersed particles is the electrical potential at the so-called slipping plane, which takes into account the binding of counter ions to the charged surface of the particles themselves. After dispersion in cell culture medium, the zeta-(ζ)-potential of GO1 was dramatically reduced to -6.4 ± 0.8 mV. Measurement of medium alone indicated that this value largely reflected the zeta-(ζ)-potential of pure cell culture medium (zeta-(ζ)-potential = 8.7 ± 1.8 mV), exhibiting a high protein and salt concentration. This was also reflected by a high conductivity of 14.9 mS/cm as compared to the conductivity of the GRM samples (between 0.07 and 0.19 mS/cm due to presence of conducting salt). Therefore, additional measurements were performed after dispersion of GRM in cell culture medium and subsequent separation of the medium by centrifugation (Table S4). For all GRM the zeta-(ζ)-potential was reduced under these conditions, reflecting a tight binding of medium constituents to the surface of the GRM.

Table S4b: Zeta-(ζ)-Potential of GNP

Zeta-(ζ)-Potential (mV)*	Water control		Acid-treated	
	With Na-cholate	Without Na-cholate	With Na-cholate	Without Na-cholate
GNP	-54.6 ± 4.1	-53.0 ± 2.0	-56.7 ± 1.8	-51.7 ± 1.5

* in ultra-pure water with 1 mM potassium chloride (KCl) background electrolyte

Further details of the XPS analysis

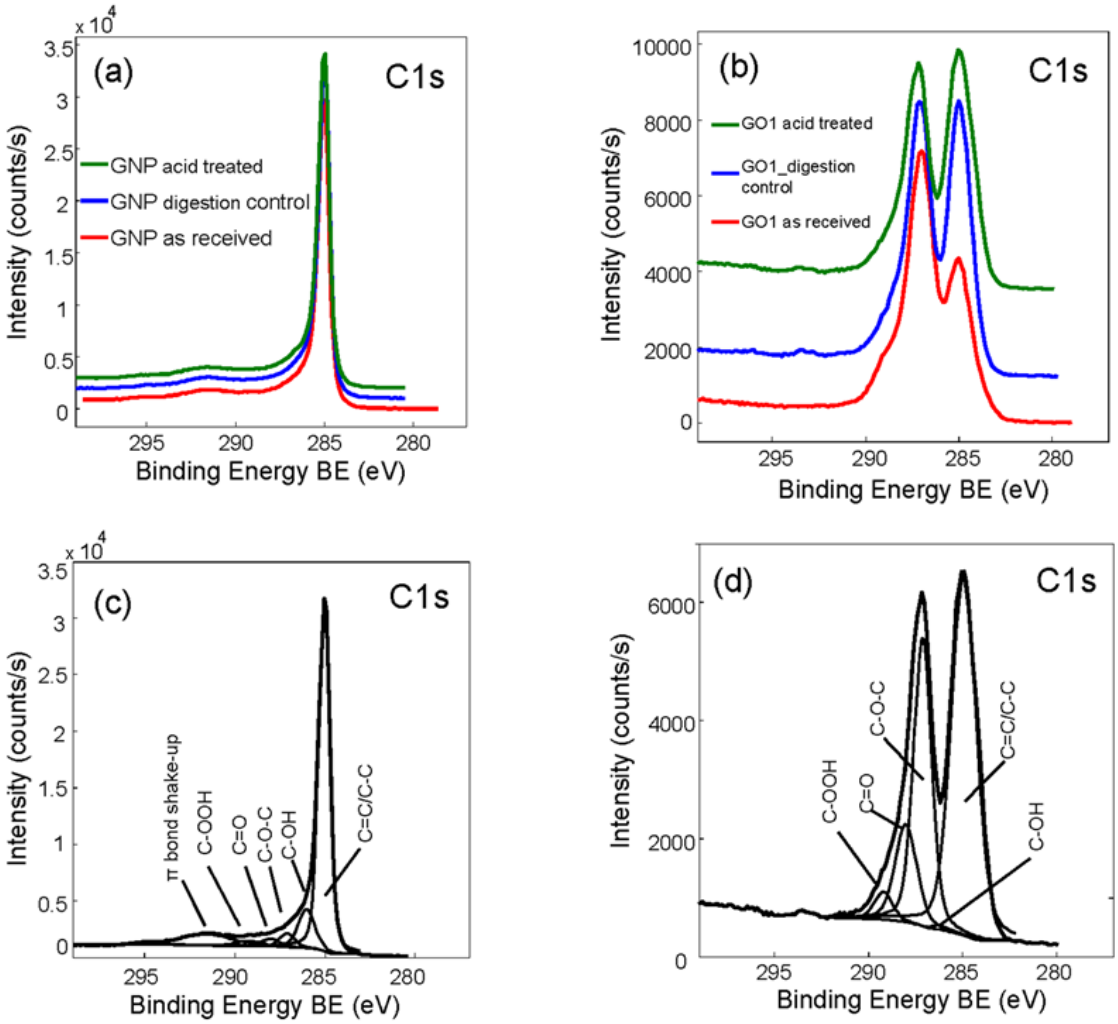

Figure S5: High-resolution elemental C1s photoelectron spectra for the GNP (a and c) and GO1 (b and d) samples. In the upper two graphs, comparisons between the samples as received (red trace), control (blue trace) and acid treated (green trace) are depicted. In the lower two graphs, the experimental spectrum (bold line) is shown together with the bands from the curve fitting with corresponding assignments as C-C/C=C, C-OH, C-O-C, C=O, C-OOH, shake-up.

Figure S5 depicts the carbon C1s high-resolution XPS spectra. In the upper graphs, the as received sample is compared to the acid treated one and the control sample (Figure S5a for GNP, Figure S5b for GO1), whereas the lower graphs show the fitting for the various oxygen functionalities (Figure S5c for GNP, Figure S5d for GO1). For the GO1 samples, high content of functional oxygen groups attached to carbon such as hydroxyl C-OH, epoxy C-O-C, carbonyl C=O, carboxyl C-OOH are observed, whereas the GNP samples are dominated by the non-functionalized carbon atoms. The spectra were deconvoluted into the expected components [1, 2], i.e. C-C, C-H, C=C bonds, C-OH bonds, C-O-C bonds, C=O bonds and C-

OOH bonds (for GNP, also the π bond shake-up peak has been considered). No changes at all in the surface chemistry have been found for the samples GNP as received, GNP control and GNP acid treated. The C1s spectral envelope (and also the O1s, not shown here) is the same for all three samples (see Figure S5a). This is in agreement with their equal C/O ratios (see Table 2). For the samples GO1 as received, GO1 control and GO1 acid treated, the C1s spectral envelope changes slightly. The amount of oxygen-functionalized compared to non-functionalized carbon atoms decreases from GO1 as received to the GO1 control and acid treated samples which might result from possible removal of oxidative debris as described by Rourke et al[3]. A further, but only minor decrease of the oxygen-functionalized groups is observed between the control and acid treated GO1 samples. Mostly the C-OH and C-O-C functionalities decrease, together with smaller reductions of the C=O and C-OOH groups. The C/O ratio increase between GO1 as received (C/O of 1.7) and the control and acid treated samples (C/O of 1.8 – 1.9) is less expressed as one could expect from the decrease of the oxygen functionalities. This is due to the presence of water in the control and acid treated GO1 samples, as found from the water peak around 536 eV in the O1s high-resolution XPS spectra (not shown here). Water can be adsorbed to GO1 interacting with oxygen groups via hydrogen bonding or can be formed due to functional oxygen group degradation [1]. Whereas no changes in the C/O ratio as well as oxygen functional groups have been seen for the GNP samples as received, control and acid treated, the observed alteration in the case of the GO1 samples can be described as only small.

Details on Raman spectroscopy:

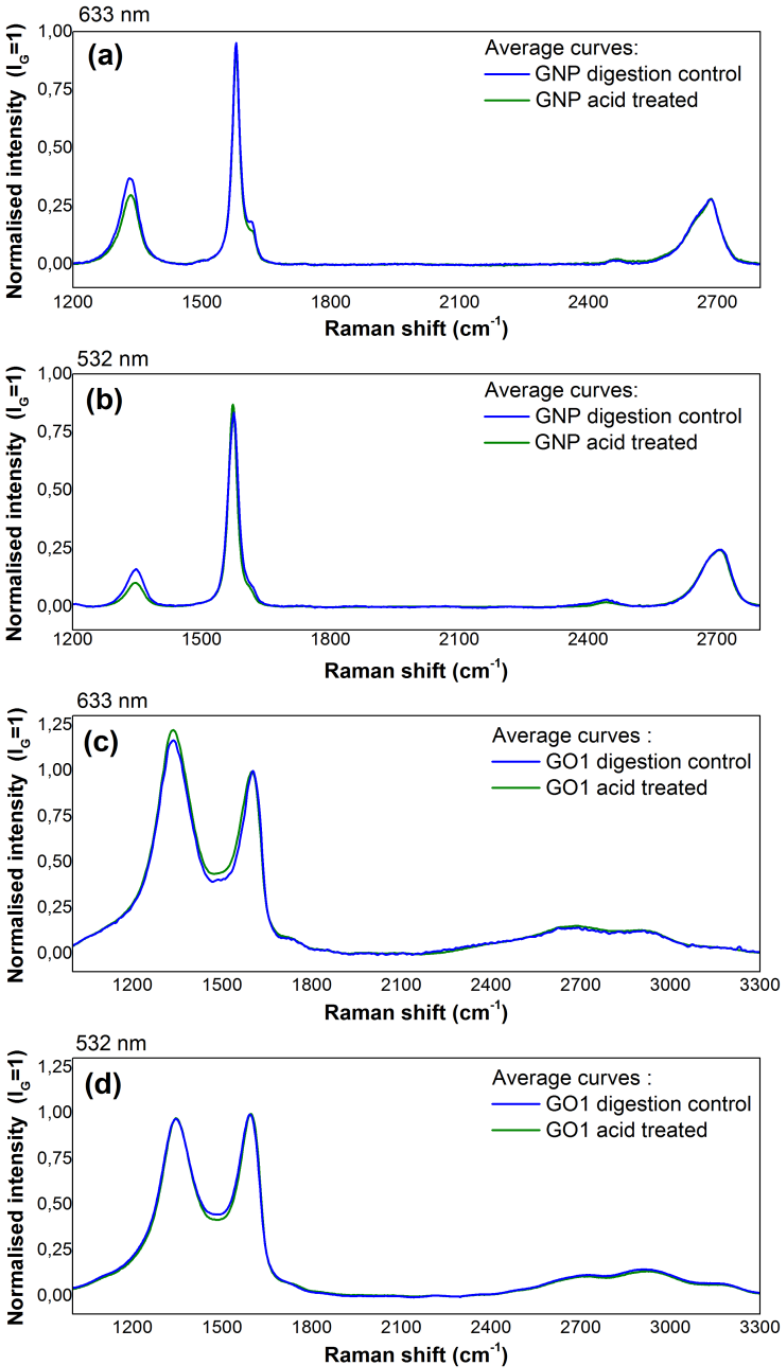

Figure S6: Comparison between Raman spectra of control and treated GRM: GNP spectra with red (a) and green lasers (b), GO1 spectra with red (c) and green lasers (d). Here, spectra are normalized so that the G band has the same intensity. In addition, each curve is an average of all the measurements carried out on the same sample at different places. Only a difference between the treated and the control GNP samples can be observed in the D band region. This one is smaller after treatment. Such a diminution is usually attributed to a decrease in the quantity of crystalline defects in the material. However in this case, it was shown by statistic t-test that it could also come from the strong heterogeneity of the starting GNP.

SEM Analysis of the interaction of acid-treated GO1 with the Caco-2 cell surface

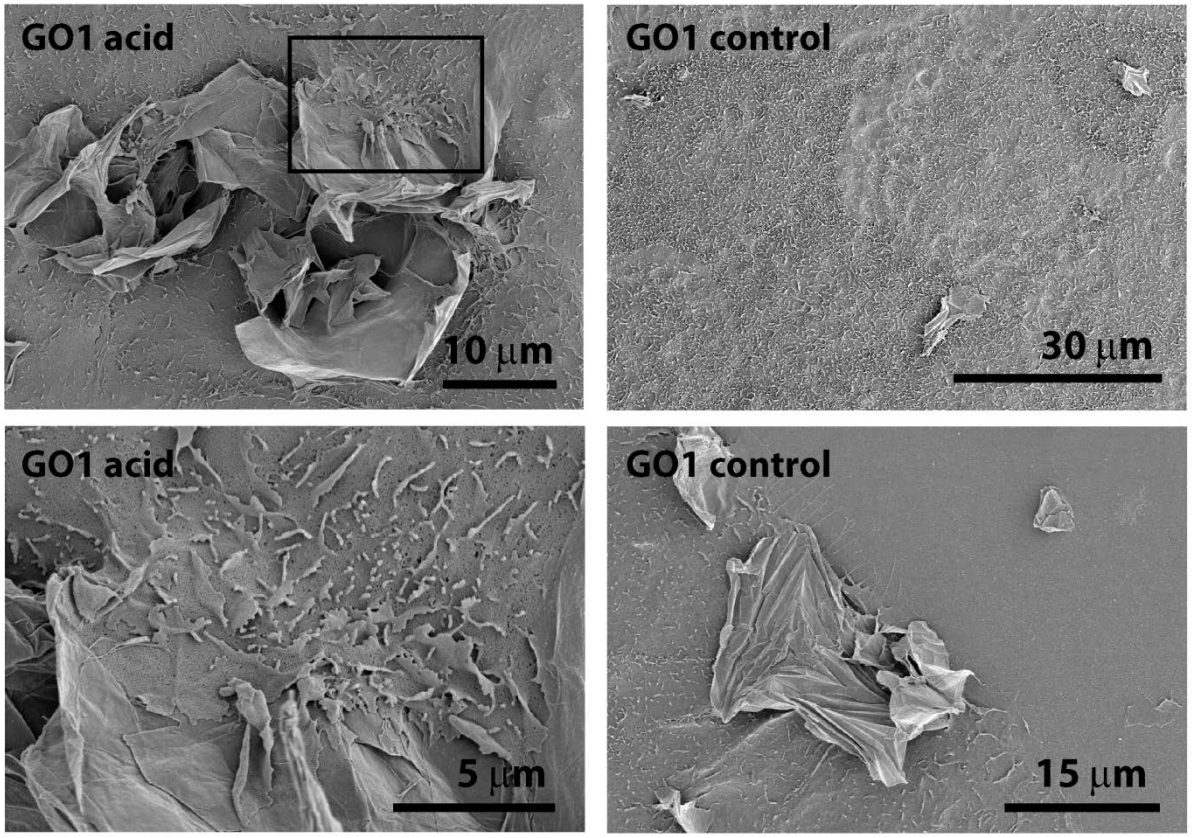

Figure S7: Representative SEM images of Caco-2 cells after exposure to 20 µg/ml acid-treated GO1 or control GO1. The black box indicates the position of the corresponding close-up view shown below. A few Caco-2 cells showed membrane protrusions and lobes in close contact to GO sheets which might be indications of cellular uptake attempts.

SEM Analysis of the interaction of acid-treated GNP with the Caco-2 cell surface

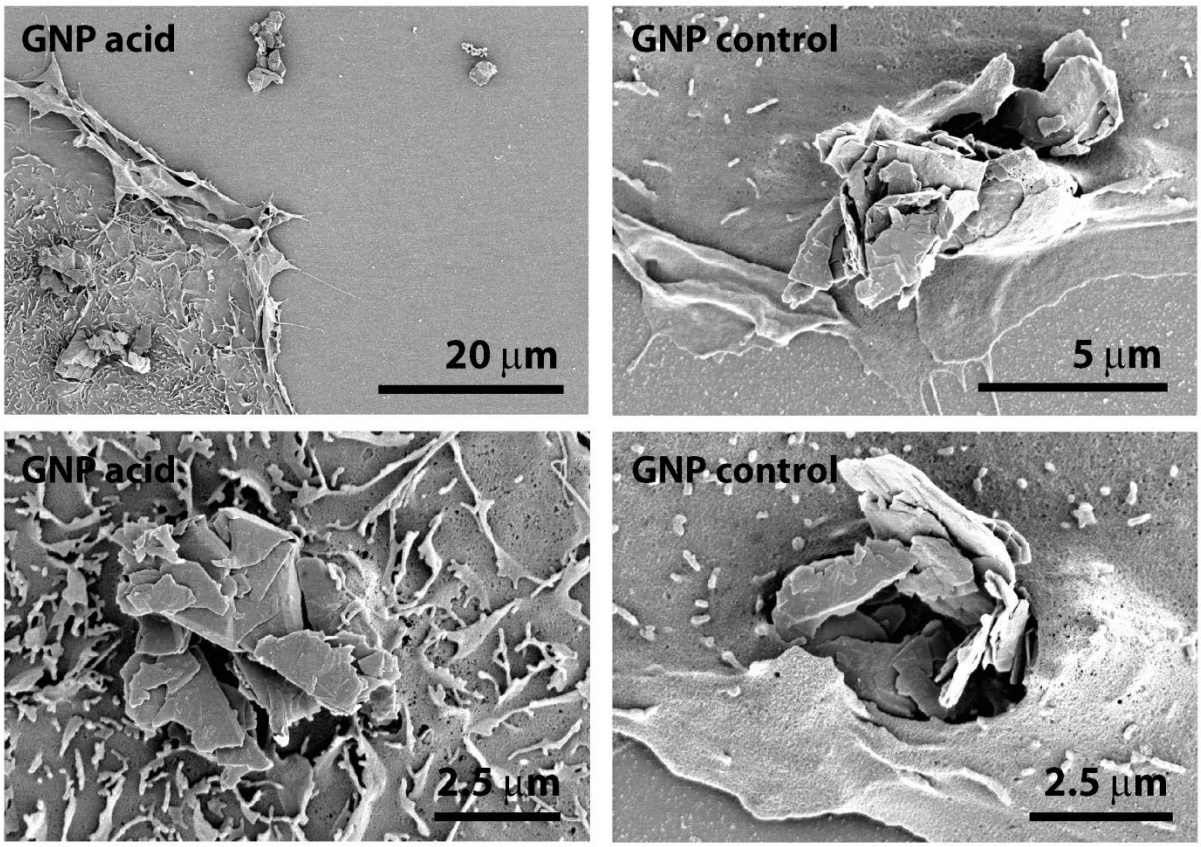

Figure S8: Representative SEM images of Caco-2 cells after exposure to 20 µg/ml acid-treated GNP or control GNP. Aggregates of GNP attached to the cell surface were primarily found near the cell borders. Caco-2 cells exhibited overgrowth of the GNP aggregates but also a few hints towards at least attempts for uptake were given.

Light microscopy – Caco-2 cells after exposure to GO1 (water-treated and acid-treated):

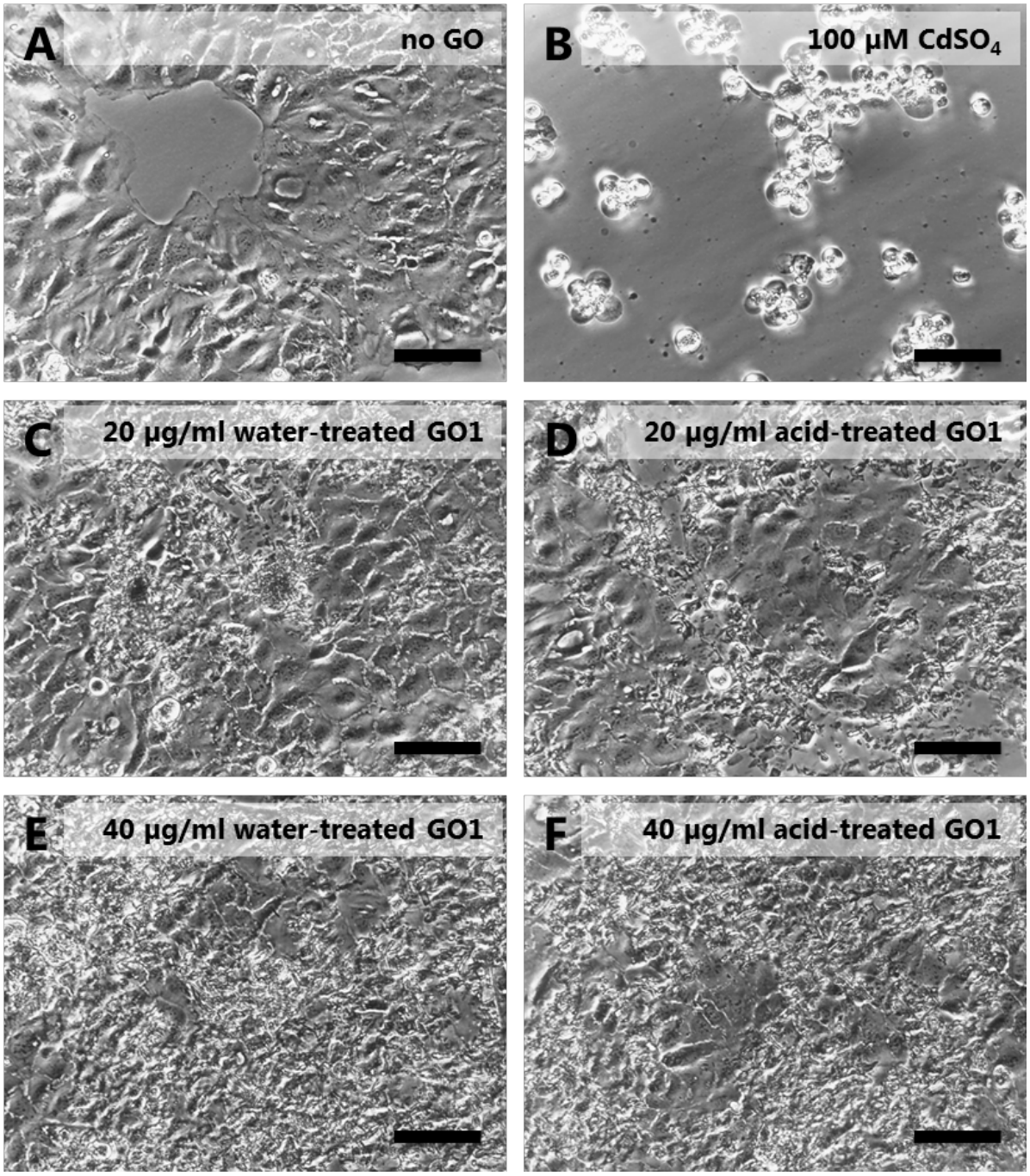

Figure S9: Representative light microscopy images of Caco-2 cells after exposure to GO1 or controls for 24 h (A = no GO1; B = negative control cells after exposure to 100 µM $CdSO_4$; C, E = control GO1 (water-treated); D, F = acid-treated GO1). Scale bar = 100 µm.

Light microscopy – Caco-2 cells after exposure to GNP (water-treated and acid-treated):

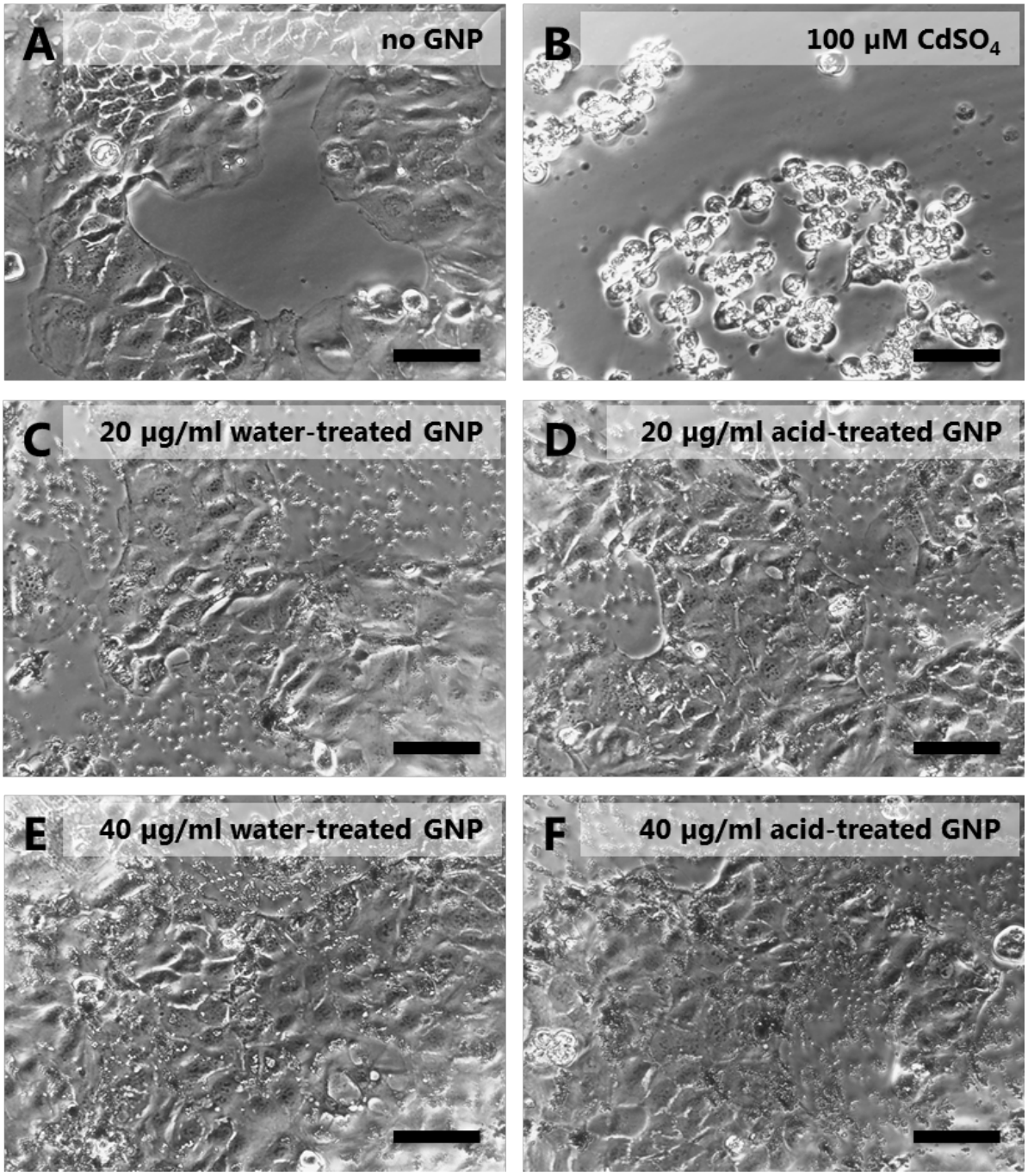

Figure S10: Representative light microscopy images of Caco-2 cells after exposure to GNP or controls for 24 h (A = no GNP; B = negative control cells after exposure to 100 µM $CdSO_4$; C, E = control GNP (water-treated); D, F = acid-treated GNP). Scale bar = 100 µm.

Absorbance of GRM samples at assay relevant wavelength:

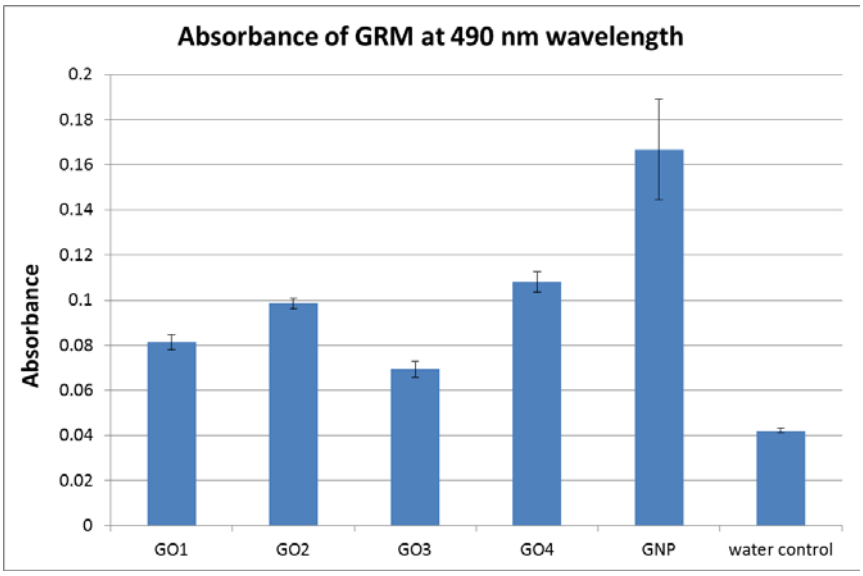

Figure S11: Mean absorbance of GRM samples (4 µg/well; equivalent to 40 µg GRM/ml) in a 96-well plate without blank correction; ultra-pure water served as negative reference/blank control. Error bars represent the standard deviation (N=2, with three replicates per sample).

DCF Assay control (cell-free): Intrinsic fluorescence of GO

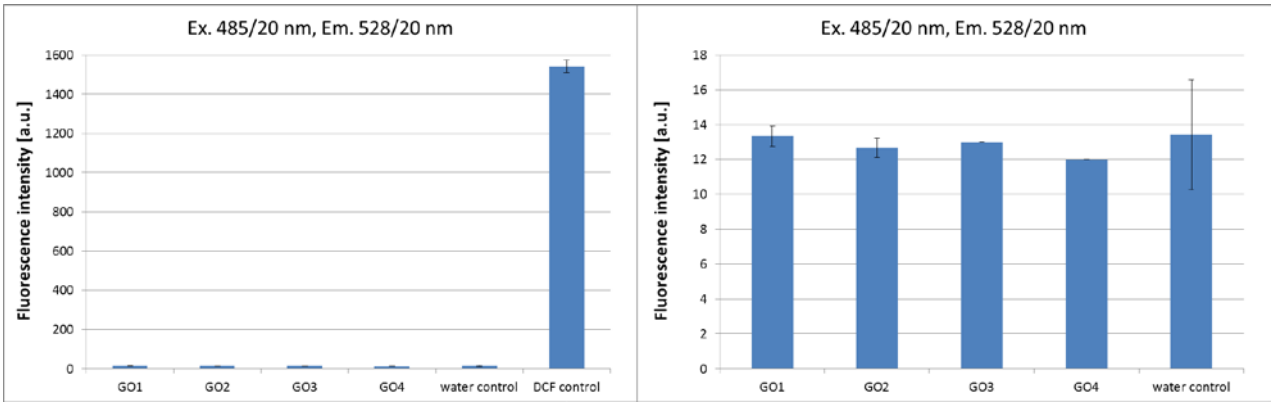

Figure S12: Mean intrinsic fluorescence [arbitrary units, a.u.] of GO samples (4 µg/well; equivalent to 40 µg GO/ml) in a 96-well plate. Intrinsic fluorescence of the four different GO was measured in the same 96-well plate, which enables direct comparison of the intensity values. DCF (2.5 µM) in ultra-pure water served as positive reference as well as ultra-pure water as negative reference. Error bars represent the standard deviation; experimental results were confirmed by independent control experiment showing similar values. All GO samples showed no intrinsic fluorescence at the standard plate reader sensitivity and filter sets applied for DCF assay.

DCF Assay control (cell-free): Intrinsic fluorescence of GNP

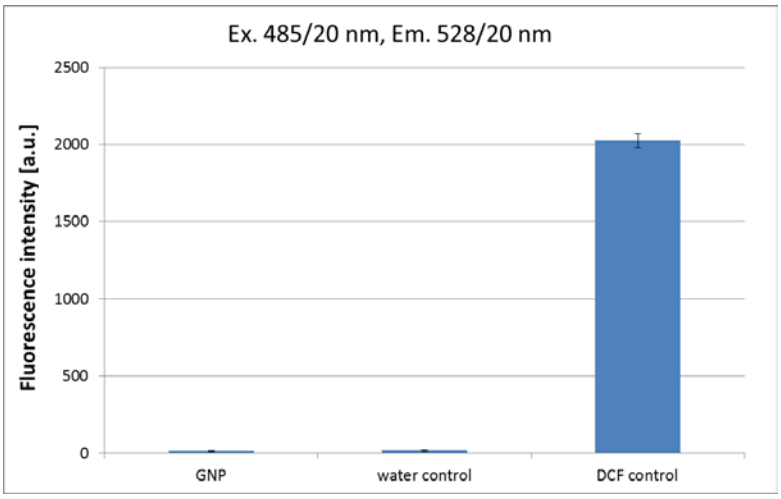

Figure S13: Mean intrinsic fluorescence [arbitrary units, a.u.] of GNP (4 µg/well; equivalent to 40 µg GNP/ml) in a 96-well plate. DCF (2.5 µM) in ultra-pure water served as positive reference as well as ultra-pure water as negative reference. Error bars represent the standard deviation; experimental results were confirmed by independent control experiment showing similar values. GNP showed no intrinsic fluorescence at the standard plate reader sensitivity and filter sets applied for DCF assay.

DCF Assay control (cell-free): Fluorescence quenching by GNP

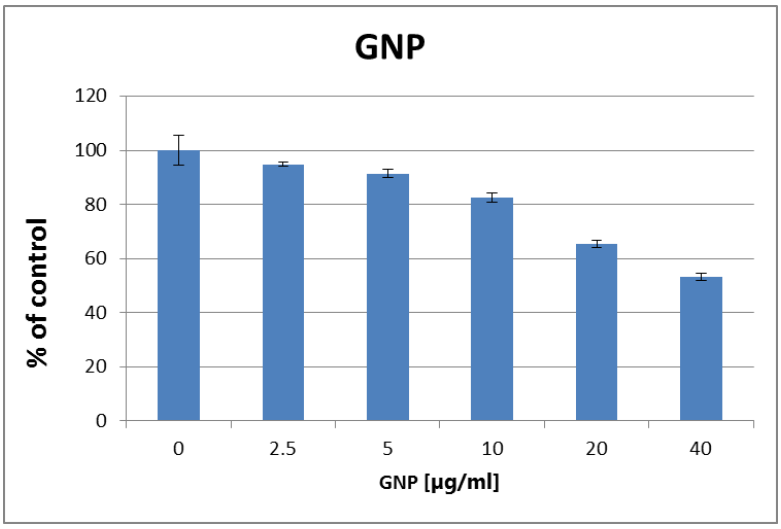

Figure S14: Mean fluorescence intensity [arbitrary units, a.u.] of DCF 2.5 µM in the absence and presence of GNP (wavelength: Ex. 485/20 nm, Em. 528/20nm). Results are presented as % of control. Error bars represent the standard deviation (n=2; three replicates per sample concentration). GNP showed concentration dependent fluorescence quenching. At the highest applied GNP concentration (40 µg GNP/ml) the measured fluorescence intensity of DCF decreased by around 50%.

DCF Assay control (cell-free): Fluorescence quenching by GO

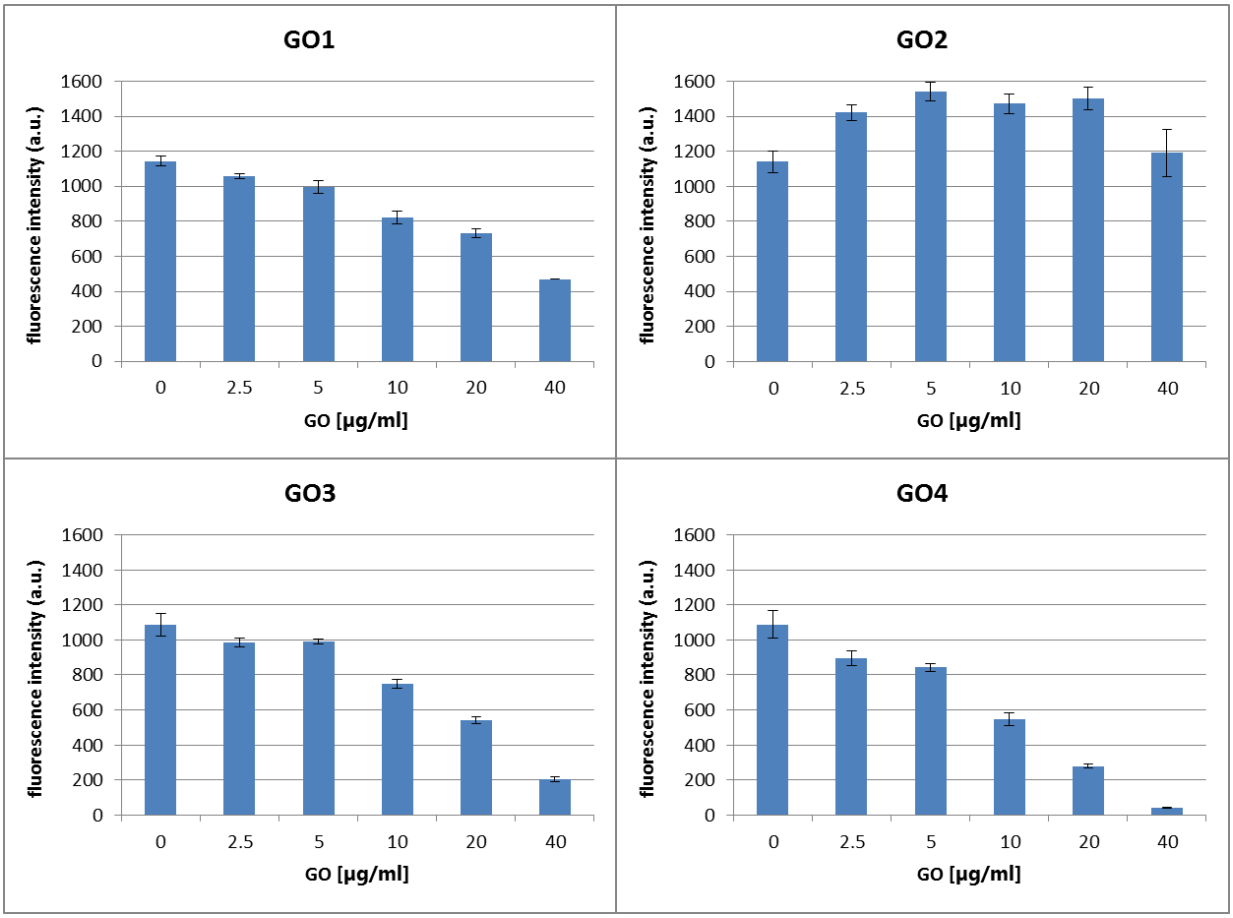

Figure S15: Mean fluorescence intensity [arbitrary units, a.u.] of DCF (2.5 µM) in the absence and presence of GO (wavelength: Ex. 485/20 nm, Em. 528/20nm). Fluorescence quenching ability of the four different GO was measured in the same 96-well plate, which enables direct comparison of the intensity values. Error bars represent the standard deviation. Experimental results were confirmed by independent control experiment showing similar results. Three GO samples (GO1, GO3 and GO4) showed concentration-dependent fluorescence quenching. In contrast, GO2 led to an increase in fluorescence intensity in the presence of GO, even at highest applied concentration of 40 µg GO/ml. Fluorescence quenching of GO2 started at a concentration between 40 and 80 µg GO/ml (data not shown).

DCF Assay control (cell-free): transformation by GRM

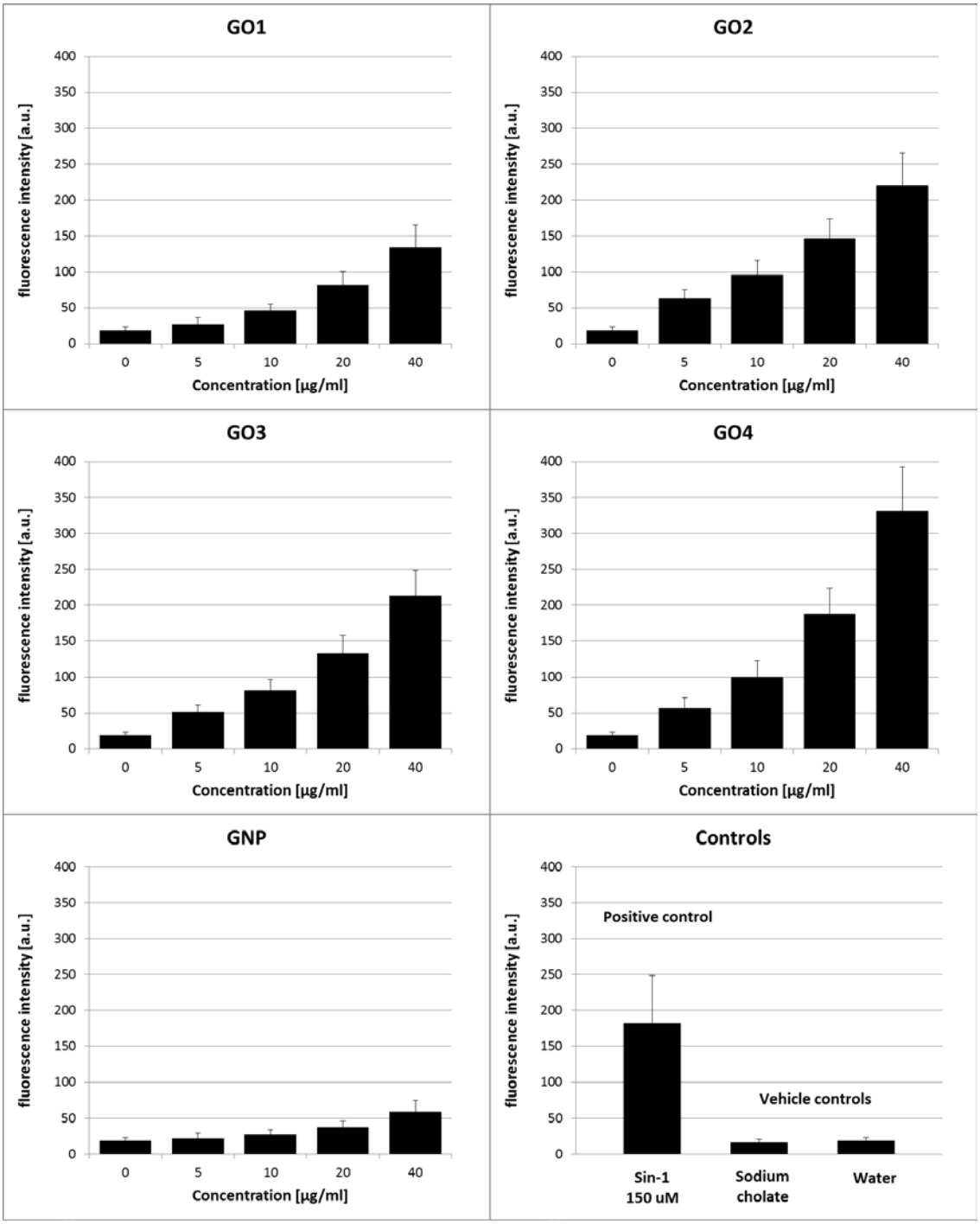

Figure S16: DCF assay performed in the absence of cells. Applied GO concentrations: 0-40 µg/ml. Sin-1 served as positive control, water and sodium cholate in water served as vehicle controls. Results presented as mean fluorescence intensity [arbitrary units, a.u.] with standard deviation of three independent experiments (with three replicates for each sample/control). Results show that the applied GRM are able to induce the formation of reactive oxygen species (ROS) in the absence of cells.

MTS Assay Interference Test (cell-free):

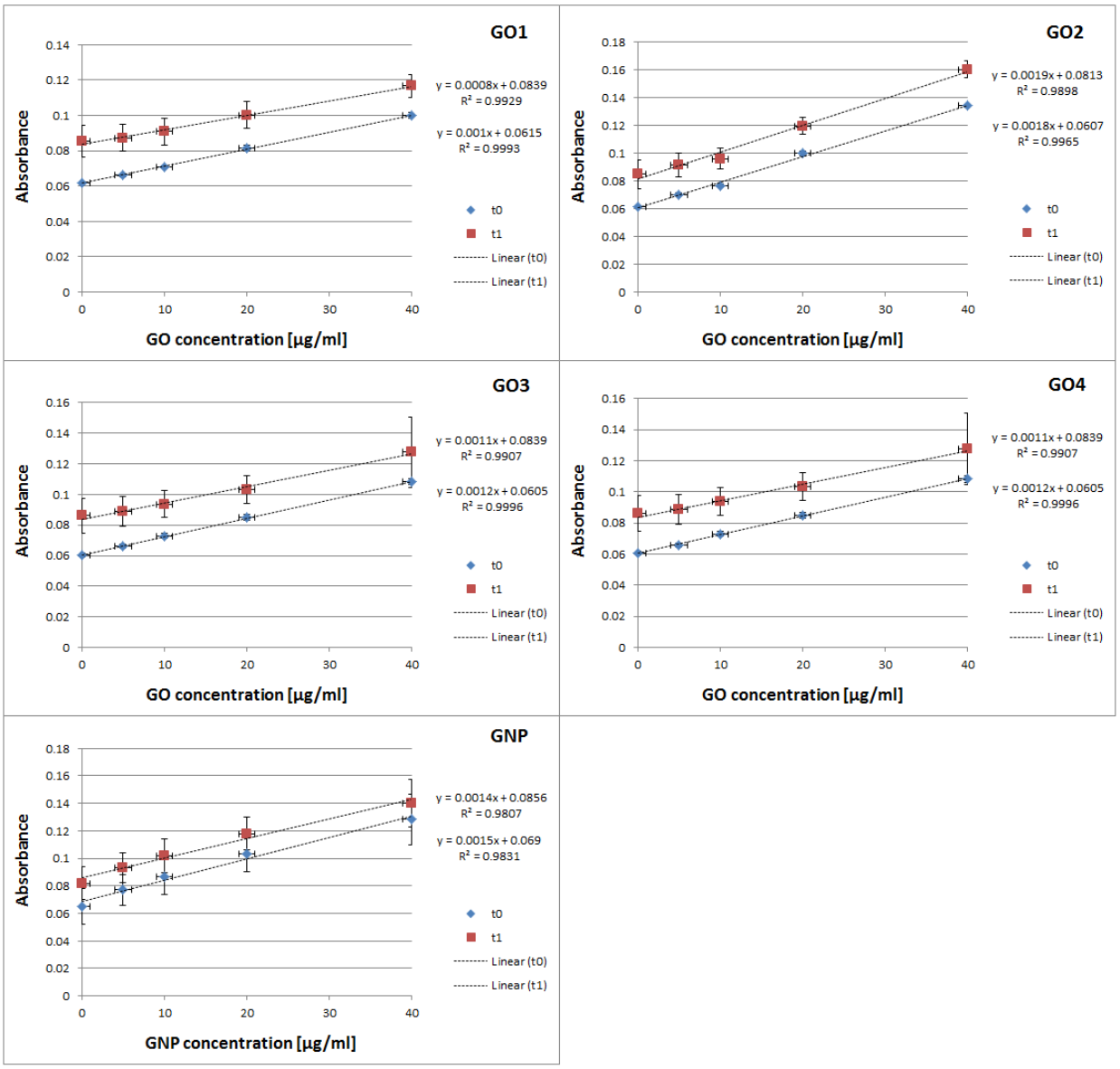

Figure S17: MTS Assay Interference Test performed in absence of cells. Results show no interference of all GRM samples with the assay reagents in a concentration range of 0-40 µg/ml GRM. The measured absorbance showed linear GRM concentration dependent increase due to the intrinsic absorbance of the GRM samples. The difference in t1 and t0 values represents the transformation of MTS reagents during 1 h incubation at 37°C. The t1/t0 ratio is relatively constant even at high concentration of 40 µg GRM/ml, which shows no interference of GRM with the assay.

References

1. L. Stobinski, B. Lesiak, A. Malolepszy, M. Mazurkiewicz, B. Mierzwa, J. Zemek, P. Jiricek and I. Bieloshapka, *Journal of Electron Spectroscopy and Related Phenomena*, 2014, **195**, 145-154.
2. S. J. Yang, J. H. Kang, H. Jung, T. Kim and C. R. Park, *Journal of Materials Chemistry A*, 2013, **1**, 9427.
3. J. P. Rourke, P. A. Pandey, J. J. Moore, M. Bates, I. A. Kinloch, R. J. Young and N. R. Wilson, *Angewandte Chemie*, 2011, **50**, 3173-3177.